

Refolding Hydrogels Self-Assembled from *N*-(2-Hydroxypropyl)methacrylamide Graft Copolymers by Antiparallel Coiled-Coil Formation

Jiyuan Yang,[†] Chunyu Xu,[†] Chun Wang,[‡] and Jindřich Kopeček^{*,†,§}

Departments of Pharmaceutics and Pharmaceutical Chemistry and of Bioengineering, University of Utah, Salt Lake City, Utah 84112, and Department of Biomedical Engineering, University of Minnesota, Minneapolis, Minnesota 55455

Received December 27, 2005; Revised Manuscript Received January 31, 2006

A novel hybrid hydrogel system based on *N*-(2-hydroxypropyl)methacrylamide copolymers was proposed. It consisted of the hydrophilic polymer backbone and a pair of oppositely charged peptide grafts. Two distinct pentaheptad peptides (CCE and CCK) were anticipated to create a dimerization motif and serve as physical cross-linkers. Consequently, the graft copolymers CCE–P and CCK–P self-assembled into hybrid hydrogels in situ; the process was modulated by the formation of antiparallel heterodimeric coiled-coils. This approach possesses an advantage to decrease the steric hindrance of the polymer backbone on the “in-register” alignment of peptide grafts. Indeed, equimolar mixtures of the graft copolymers, CCE–P/CCK–P, have been observed to self-assemble into hydrogels in PBS solution at neutral pH at concentrations as low as 0.1 wt %. Circular dichroism spectroscopy, sedimentation equilibrium experiments, and microrheology revealed that the self-assembly process corresponded to the two-stranded α -helical coiled-coil formation between CCE and CCK. Moreover, the formation of hybrid hydrogels was reversible. Denaturation of the coiled-coil domains with guanidine hydrochloride (GdnHCl) solutions resulted in disassembly of the hydrogels. Removal of GdnHCl by dialysis caused coiled-coil refolding and hydrogel reassembly. Scanning electron microscopy results demonstrated that the concentration of the graft copolymers had a significant impact on the structure and morphology of self-assembled hydrogels.

Introduction

Supramolecular biological structures are often constructed through self-assembly of natural polymeric building blocks. Molecular self-assembly has become a rapidly advancing area of research not only because of fundamental interest but also due to the practical importance in building highly sophisticated, functional biomaterials.^{1–10}

Self-assembly of proteins and peptides has generated most of the structural and functional biological systems, such as actin filaments of the cytoskeleton, and is characterized by distinct features. First, the assembly process is highly specific and is mediated by molecular recognition and binding among polypeptide building blocks. Second, it is a stimuli-responsive process in which external signals, such as pH and a molecular ligand, can trigger or terminate the assembly. Finally, the assembly and disassembly processes are mostly reversible, allowing precise, dynamic control of the material's structure and properties.

The coiled-coil,^{11–13} one of the basic folding domains of native proteins, has been widely used in the self-assembly of biological and synthetic materials.^{14–21} It consists of two or more α -helices winding together and forming a superhelix. Its primary structure is characterized by a heptad repeating sequence, (abcdefg)_{*n*}, where the a and d positions are usually hydrophobic amino acid residues. The number of strands can alter from 2 to 5; the orientation between the helices can be parallel

or antiparallel. Such structural variations result in different biological functions. The current stage of knowledge will permit the design of a coiled-coil with predetermined properties such as stability, orientation, and specificity (homodimer/heterodimer).^{11–13,18,22–29} The coiled-coil has already been used in a number of applications including affinity purification,³⁰ multimeric antibodies,³¹ epitope display,³² nanoparticle assembly,³³ etc.

Recently, coiled-coils have been used to drive the assembly of genetically engineered block protein hydrogels^{14,18} and hybrid hydrogels consisting of water-soluble synthetic polymers and engineered protein domains.^{15,34,35}

Previous work in our laboratory developed a new strategy of hybrid hydrogel synthesis.¹⁵ The genetically engineered coiled-coil protein motifs were noncovalently attached to a hydrophilic synthetic *N*-(2-hydroxypropyl)methacrylamide (HPMA) copolymer backbone. The physical crosslinking was established by self-assembly of the coiled-coil domains. A temperature-induced hydrogel collapse was found which corresponded to the structural transition of the coiled-coil domains from an elongated helix to an unfolded state. Here, a modified approach of self-assembly of graft copolymers into hybrid hydrogels was proposed, which involved two oppositely charged peptide grafts. We hypothesize that the peptide grafts would form heterodimers with an antiparallel orientation. As a result, HPMA copolymers containing coiled-coil peptide grafts are expected to form gels in situ via self-assembly. The homogeneity of the self-assembled hybrid hydrogels will be enhanced due to not only the uniqueness of interchain dimer formation but also the decreased steric hindrance of the polymer backbone on the “in-register” alignment of the peptide heterodimers. This study will increase the fundamental understanding of new tunable peptide–synthetic

* To whom correspondence should be addressed. E-mail: jindrich.kopecek@m.cc.utah.edu.

[†] Department of Pharmaceutics and Pharmaceutical Chemistry, University of Utah.

[‡] University of Minnesota.

[§] Department of Bioengineering, University of Utah.

polymer hybrid materials that are of potential utility as stimuli-responsive biomaterials.

Experimental Section

Materials. Side-chain-protected Fmoc-amino acids, 2-chlorotrityl resin, benzotriazole-1-yl-oxy-tris-pyrrolidinophosphonium hexafluorophosphate (PyBOP), and 1-hydroxybenzotriazole (HOBt) were purchased from Novabiochem (San Diego, CA). Dimethyl sulfoxide (DMSO; 99.9% pure) was purchased from EMD Chemicals (Gibbstown, NJ). Trifluoroacetic acid (TFA), trifluoroethanol (TFE), dimethylformamide (DMF), methanol, and piperidine were purchased from VWR International (West Chester, PA). 2,2'-Azobisisobutyronitrile (AIBN) and succinimidyl *trans*-4-(maleimidylmethyl)cyclohexane-1-carboxylate (SMCC) were from Soltech Ventures (Beverly, MA). (3-Aminopropyl)methacrylamide was from Polysciences (Warrington, PA), and HPMA was synthesized as previously described.³⁶

Peptide Synthesis and Purification. All peptides were synthesized using solid-phase methodology and the manual Fmoc/tBu strategy on 2-chlorotrityl resin as described previously.²¹ The resulting dry resin-bound peptides were cleaved and the side chains deprotected using TFA/H₂O/ethanedithiol/triisopropylsilane (94.5:2.5:2.5:1) cocktail. Crude peptides were precipitated with diethyl ether. Peptide purification was carried out by RP-HPLC using a semipreparative Zorbax 300SB-C18 column (250 × 9.4 mm, 5 μm particle size, 300 Å pore size) from Agilent Technologies. The peptides were eluted with a linear gradient at a flow rate of 2 mL/min, where buffer A was 0.1% TFA in water and buffer B 0.1% TFA in acetonitrile. The purity of the peptide in the fractions was verified with analytical RP-HPLC. Fractions were pooled and lyophilized. The identity of the peptides was ascertained by MALDI-TOF mass spectrometry (Voyager-DE STR Biospectrometry Workstation, Perseptive Biosystems, Framingham, MA).

Synthesis of HPMA Graft Copolymers Containing Coiled-Coil Domains. The synthetic procedure consisted of three steps: first, a copolymer of HPMA and *N*-(3-aminopropyl)methacrylamide (MA-NH₂) was prepared by radical copolymerization in methanol at 50 °C with AIBN as the initiator. Then, the amino groups at the side chain termini were converted to maleimide groups (polymer precursor) by reaction with a heterobifunctional reagent, SMCC. Finally, the coiled-coil peptides flanked with a cysteine residue at the N-terminus were attached to the polymer side chains via thioether bonds.

Copolymerization of HPMA with MA-NH₂. A mixture of HPMA (3.22 g, 22.5 mmol), MA-NH₂ (0.45 g, 2.5 mmol), and AIBN (0.177 g) was dissolved in 25.5 g of methanol, bubbled with nitrogen for at least 5 min, sealed in an ampule, and kept for 24 h at 50 °C. The product was dialyzed against water and freeze-dried. The yield was 53.4%. The molecular weight and molecular weight distribution of the copolymer were measured on an ÄKTA FPLC system (Amersham Pharmacia Biotech) equipped with UV and RI detectors using a Superose 6 HR10/30 column with PBS (pH 7) as the mobile phase. The average molecular weights were calculated using a calibration with polyHPMA fractions. The content of amino groups in the copolymer (P-NH₂) was 9.64 mol %, as determined by a ninhydrin assay (feed content 10 mol %).³⁷

Synthesis of HPMA Copolymer with Side Chains Terminated in Maleimide (Polymer Precursor). A mixture of 0.5 g of P-NH₂ (0.329 mmol of NH₂) and SMCC (0.1650 g, 0.493 mmol) was dissolved in 4 mL of DMF and kept at room temperature overnight in the presence of triethylamine. The product was precipitated into acetone/ether (3:2), filtered, redissolved in methanol, precipitated into acetone again, filtered, and dried under vacuum. The amount of maleimide in the copolymer was 6.4 mol % as determined by a modified Ellman assay.³⁸

Attachment of Peptides to the Polymer Backbone. An aqueous solution (4 mg/100 μL) of the peptide (CCE or CCK) was mixed with a polymer precursor solution (typically 5 mg/mL). The reaction mixture was kept at room temperature for 2 h. The products were purified by RP-HPLC equipped with a semipreparative column, and the final products were confirmed by analytical RP-HPLC and SDS-PAGE.

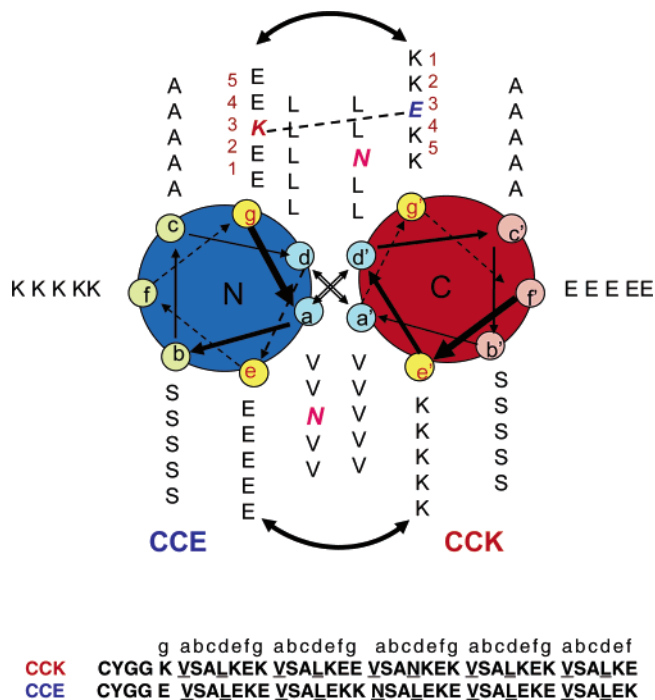


Figure 1. Helical wheel representation of two-stranded, antiparallel α -helical coiled-coils formed by the dimerization of CCE and CCK. The view is shown looking down the superhelical axis from the N-terminus of CCE and from the C-terminus of CCK. CC denotes the coiled-coil peptides. E and K denote peptides in which most of the e and g positions are occupied by either glutamic acid or lysine, respectively. The sequences are written in the one-letter amino acid code. Positions a and d of the heptad repeat are underlined and form the hydrophobic core of the coiled-coil.

In the following, the conjugates were designated as CCE-P and CCK-P (P is the HPMA copolymer backbone). The amount of grafts was determined by amino acid analysis. The samples were hydrolyzed with 6 N HCl at 120 °C for 24 h in sealed ampules. HCl was then removed under reduced pressure, and the samples were further dried under vacuum. Then they were precolumn derivatization with 4-phthalaldehyde and analyzed by HPLC with fluorescence detection [excitation, 229 nm; emission, 450 nm; gradient elution with buffer A (0.05 M sodium acetate, pH 6.0) and buffer B (70% methanol in buffer A)].

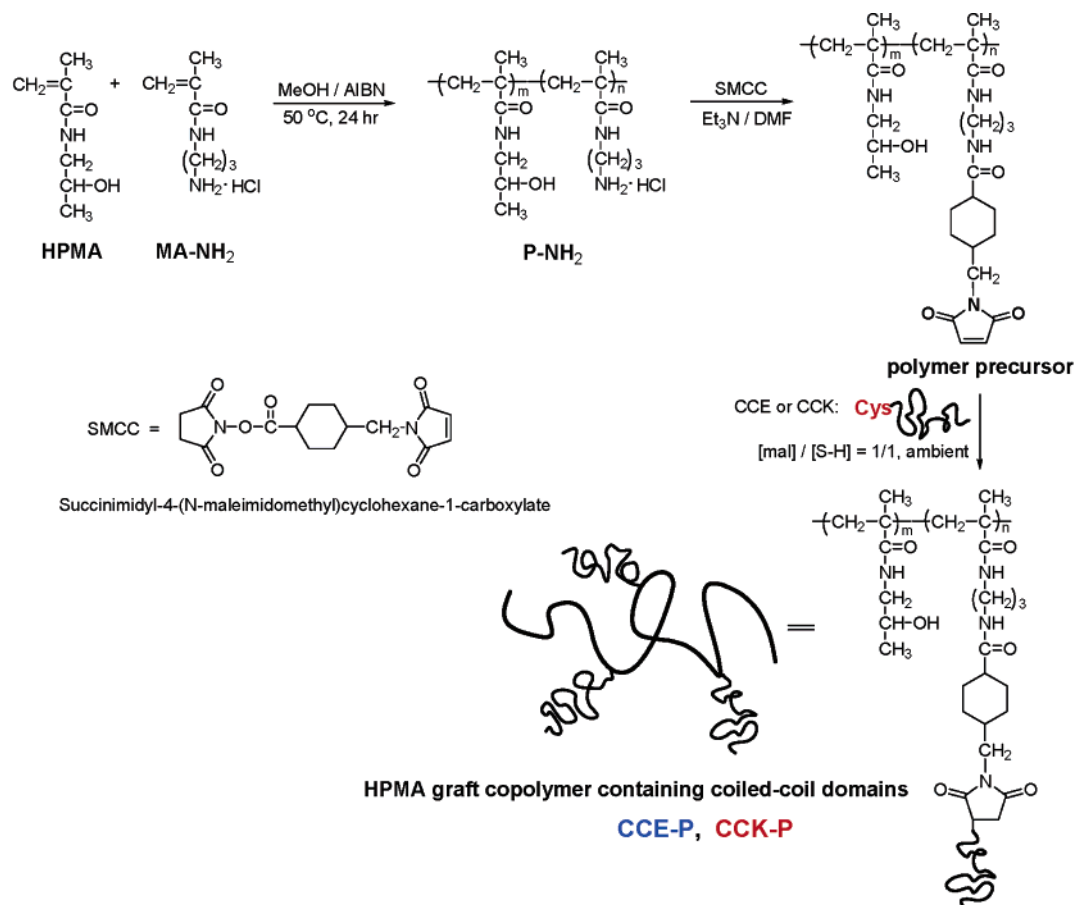
Circular Dichroism Spectroscopy. Circular dichroism (CD) spectra were collected on an Aviv 62DS CD spectrometer with a thermoelectric temperature-control system. The samples were prepared at a concentration of 0.45 mg/mL (approximately 100 μM) in benign buffer (50 mM Na₂HPO₄/NaH₂PO₄, 100 mM KCl, pH 7.0), unless otherwise stated. Wavelength scans were recorded at 1 nm intervals and a 5 s averaging time at each step from 250 to 200 nm using a 0.1 cm path length quartz cuvette. The spectra obtained were averaged from three consecutive scans and subtracted from the background. Ellipticity is reported as the mean residue ellipticity ($[\theta]$, (deg·cm²)/dmol) and calculated as

$$[\theta] = [\theta]_{\text{obsd}}(\text{MRW})/(10lc)$$

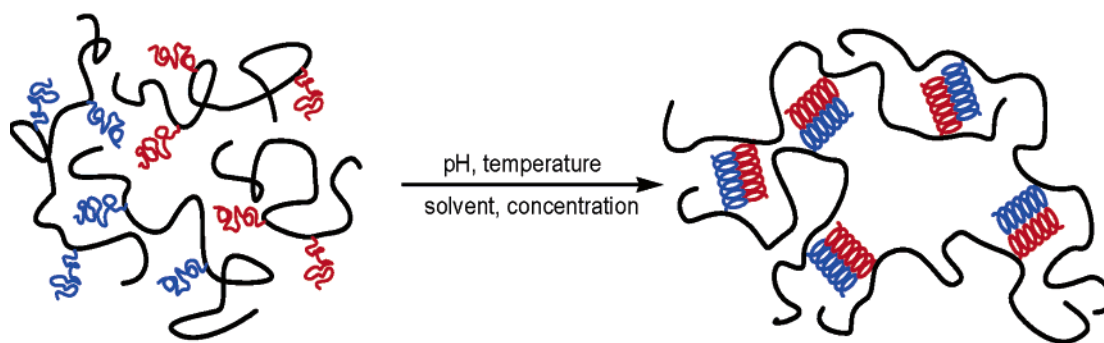
where $[\theta]_{\text{obsd}}$ is the ellipticity measured in millidegrees, MRW is the mean residue molecular weight of the polypeptide (molecular weight of the peptide divided by the number of amino acid residues), l is the optical path length of the cell (cm) (0.1 cm in our case), and c is the peptide concentration (mg/mL).²⁴

The thermal stability of the samples was determined by monitoring the change of ellipticity at 222 nm as a function of temperature from 4 to 97 °C at 3 °C per step. For each step, the sample was equilibrated for 1.5 min followed by 30 s of data point averaging.

Guanidium chloride (GdnHCl) denaturation studies were carried out by monitoring the ellipticity at 222 nm. Mixtures were prepared from



A



B

Figure 2. (A) Synthesis of HPMA graft copolymers and (B) schematic representation of hydrogel formation through antiparallel heterodimeric coiled-coil association.

peptide stock solutions in buffer and a solution of 8 M GdnHCl in the same buffer. The fraction folded was calculated using the equation

$$F_F = ([\theta] - [\theta]_D) / ([\theta]_F - [\theta]_D)$$

where $[\theta]$ is the observed molar ellipticity and $[\theta]_F$ and $[\theta]_D$ are the ellipticities of the folded and denatured states, respectively. The upper and lower linear regions were extrapolated to get the $[\theta]_F$ and $[\theta]_D$ values characteristic of the transition region.²⁴

Analytical Ultracentrifugation. Sedimentation equilibrium experiments were performed on a Beckman Optima XL-A analytical ultracentrifuge fitted with an AnTi60 rotor, and six-channel cells of 12 mm optical path length were employed (three solution/solvent pairs). CCE, CCK, and an equimolar mixture of CCE/CCK were dissolved

in benign buffer (50 mM Na₂HPO₄/NaH₂PO₄, 100 mM KCl, pH 7) with 0.2 mM DTT and dialyzed against the same buffer overnight. Final concentrations were assayed by Micro BCA (bicinchoninic acid) protein assay. Three different loading concentrations of 50, 75, and 100 μ M were used. Samples were centrifuged to equilibrium with a rotor speed of 60000 rpm at 20 $^\circ$ C, and the absorbance was recorded at 230 nm (amide). Equilibrium was confirmed by the overlays between scans taken at 4 h intervals. A baseline scan at a nonabsorbing wavelength (360 nm) was taken once the equilibrium was attained. The data were processed and analyzed with a nonlinear least-squares curve-fitting algorithm in the program NONLIN. The values of ν -bar for each protein were calculated from the amino acid sequence.³⁹

Hydrogel Preparation. Freeze-dried HPMA copolymers grafted with peptides, CCE-P and CCK-P, were dissolved in benign buffer

and dialyzed against the same buffer separately for at least 6 h. Then an equimolar mixture of CCE–P/CCK–P solutions was incubated at room temperature until self-assembling gelation occurred.

Microrheology. Microrheological measurements were performed as previously described¹⁸ by dispersing a small amount of 0.5 μm fluorescently labeled amidine-modified polystyrene microspheres into polymer solutions. Briefly, the samples were sealed between a microscope slide and a glass coverslip with Cyto seal 60. The Brownian motion of the tracer particles was captured by digital video microscopy (Nikon Eclipse E800) with a 100 \times oil-immersion objective and a CCD camera (Dage-MTI, DC330) with an exposure time of 2 ms. For each sample, 3000 images were recorded at intervals of 33 ms using StreamPix software (Norpix, Montreal, Canada) and analyzed with IDL software (Research Systems Inc., Boulder, CO). Particle trajectories were extracted and analyzed using algorithms developed and kindly provided by the Weitz group.⁴⁰

Scanning Electron Microscopy (SEM). Hydrogel samples, prepared as described above, were equilibrated with DI water to remove PBS, shock-frozen by immersion into liquid nitrogen, and freeze-dried. The dry samples were then fixed on aluminum stubs and sputtered with gold for 40 s. The morphologies were studied using a scanning electron microscope (Hitachi S-2460N SEM instrument).

Results and Discussion

Peptide Design. Two pentaheptad sequences with opposite charges (CCE and CCK, Figure 1) were designed on the basis of generally accepted principles governing coiled-coil conformation with the goal of achieving an antiparallel heterodimeric conformation.^{24–29} Briefly, three major stabilizing interactions were taken into account: the hydrophobic interactions in the core, electrostatic attractions across the interface, and helical propensity effects. Valine and leucine were chosen for the a and d positions, respectively, because of their high hydrophobicity, ability to pack into the core, and propensity to promote formation of dimeric coiled-coils in numerous leucine zipper mutants. Charged residues were placed at positions e and g. Potentially attractive or repulsive electrostatic interactions between these residues have been shown to influence partner strand specificity and orientation preference. Glutamic acid occupied the e and g positions in one strand (CCE), while in the other strand (CCK) lysine was placed at the e and g positions. This design ensured that the formation of the two potential homodimers was thermodynamically less probable due to destabilization by electrostatic repulsions.^{11,26,28,29} Moreover, a single residue at the g position of the fourth heptad in each strand was substituted with the oppositely charged one. The orientation preference was thus improved, because all potentially attractive interactions are expected in the antiparallel alignment. Positions b and c were filled with serine and alanine residues, respectively. Uncharged residues were used in these positions to avoid electrostatic interactions with adjacent residues at positions e and g. Serine was chosen to enhance solubility. Alanine possesses high helical propensity and was expected to promote helix formation. Lysine was chosen for position f in the CCE coil and glutamic acid in the CCK coil to balance the net charge of each peptide and increase solubility. It was reported that buried polar interactions played a key role in the structural specificity of coiled-coils; in particular, a single buried polar interaction at the hydrophobic interface of the helices of a coiled-coil was sufficient to impose an antiparallel alignment.^{41,42} Therefore, asparagine residues were placed at the a and d' positions of the third heptad of the CCE coil and CCK coil, respectively. Finally, the coiled-coil sequences were flanked at the N-terminus with a Cys–Tyr–Gly–Gly tetrapeptide spacer

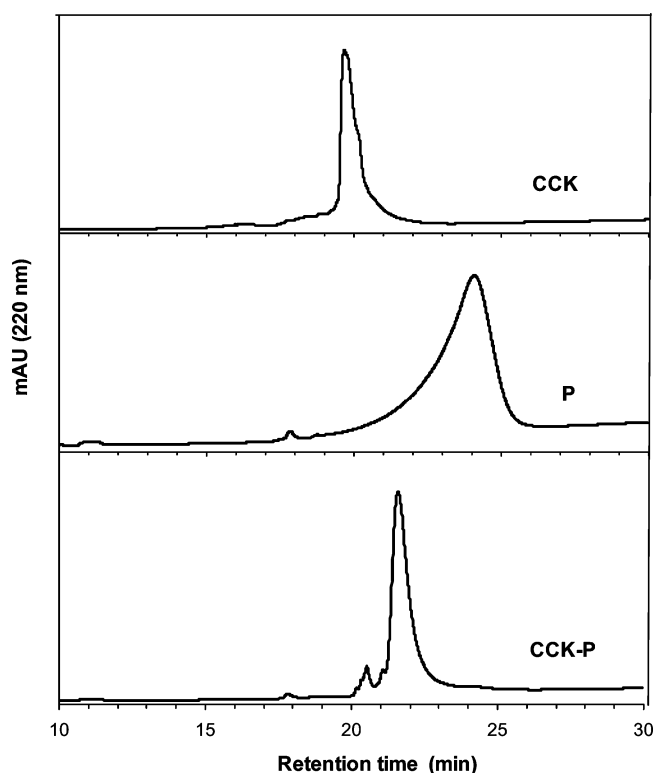


Figure 3. Analytical reversed-phase HPLC chromatograms of the CCK peptide, the HPMA copolymer precursor (P), and their conjugate, CCK–P. The chromatogram was developed using a ZOBRAx C18 column (250 \times 4.6 mm) with an Agilent 1100 system at a flow rate of 1 mL/min using a gradient of 2–60% acetonitrile over 30 min.

Table 1. Characterization of HPMA Copolymers Containing CCE/CCK Grafts^a

name	peptide content (wt %)		no. of grafts per macromolecule
	calcd	found	
CCE–P	62.4	50.8	19.4
CCK–P	60.1	56.1	24.2
CCE–P/CCK–P	mixture formed by a 1:1 mole ratio of CCE–P and CCK–P		

^a The polymer backbone $M_n = 79000$, $M_w/M_n = 1.4$, and $[\text{mal}] = 3.96 \times 10^{-7}$ mol/mg of polymer.

to further decrease the steric hindrance of the polymer backbone on the formation of antiparallel heterodimers and provided an attachment point.

The peptides CCK and CCE were prepared manually using the standard Fmoc strategy. Part of CCE was obtained from the Emory University Microchemical Facility. After purification, the structure was confirmed by MALDI-TOF MS and amino acid analysis. The molecular weights of both CCE and CCK were in good agreement with the theoretical values (calculated/ found: CCE, 4196.7/4197.3; CCK, 4180.4/4180.2).

Synthesis and Characterization of HPMA Graft Copolymers. The synthesis of HPMA copolymers containing coiled-coil grafts is outlined in Figure 2A. The maleimide group-bearing polymer precursor was first prepared by the reaction of amine-containing HPMA copolymer with SMCC in the presence of triethylamine in DMF. The peptides CCE and CCK were attached to the polymer backbone via thioether bonds formed by the reaction of maleimide with cysteine at the N-termini of CCE and CCK. These peptide grafts were expected to form antiparallel heterodimers under suitable conditions and to provide the pathway for hydrogel formation as shown in Figure 2B. The polymer analogous reaction of the polymer

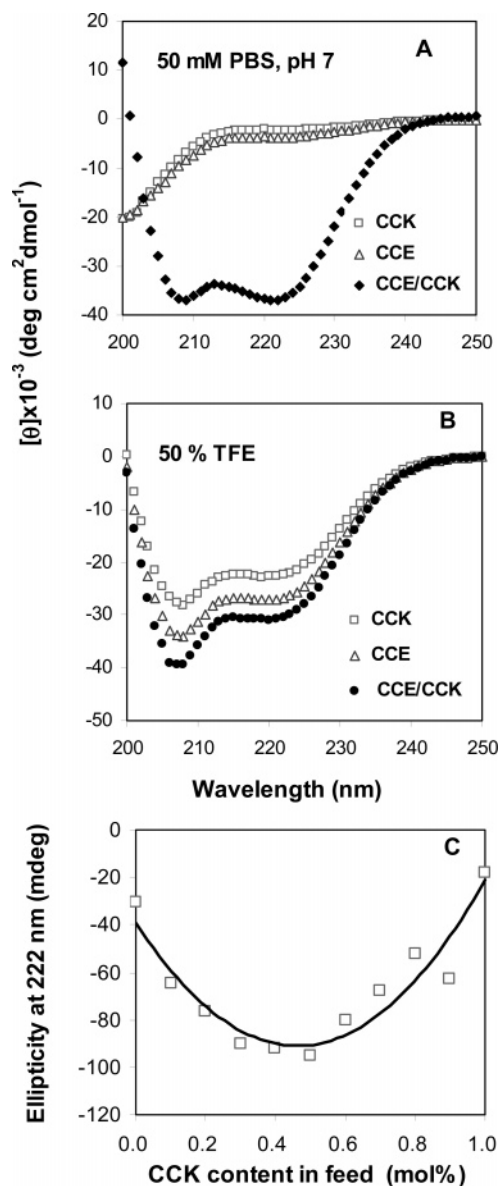


Figure 4. CD spectra of CCK, CCE, and their equimolar mixture CCE/CCK with (A) and without (B) 50% TFE of the α -helix-inducing solvent TFE. (C) Effect of the mole ratio in the mixture on the ellipticity at 222 nm (no TFE). The spectra were recorded at 25 °C in 50 mM Na₂HPO₄/NaH₂PO₄, 100 mM KCl, pH 7.0. All peptide concentrations were approximately 0.45 mg/mL (100 μ M).

precursor with cysteine at the N-termini of CCE and CCK was monitored with RP-HPLC (Figure 3). Unreacted species were removed by RP-HPLC. The final products were confirmed by analytical HPLC and SDS-PAGE; no free peptide was detectable (data not shown). The amount of grafts, determined by amino acid analysis, is given in Table 1.

Heterodimeric Coiled-Coil Formation. The secondary structure of the peptides CCE and CCK was evaluated by CD spectroscopy. Because of a high net charge, CCE and CCK individually were predominantly unfolded in neutral aqueous solution, while their equimolar mixture CCE/CCK formed a stable heterodimer, as demonstrated by CD spectra displaying negative minima at 222 and 208 nm (Figure 4A).²⁷ These observations were supported by the results of equilibrium sedimentation studies (Table 2). There was no association for isolated peptides CCE and CCK in a neutral condition and at room temperature. The apparent molecular weight of the equimolar mixture CCE/CCK indicated dimer formation.

Table 2. CD Spectroscopic Data and Association Analysis by AUC

	α -helix content ^a (%)		$[\theta]_{222}/[\theta]_{208}$		AUC ^b	
	PBS	50% TFE	PBS	50% TFE	M_{wapp}	oligomer- ation
CCE	11	87	0.40	0.78	4485	monomer
CCK	6	63	0.26	0.78	4910	monomer
CCE/CCK	100	76	1.00	0.79	7830	dimer

^a The helical content (%) was calculated from the ratio of the observed $[\theta]_{222}$ divided by the predicted molar ellipticity $\times 100$.⁴⁰ The predicted molar ellipticity was calculated from the equation $[\theta]_{222} = (-40 \times 10^3)(1 - 4.6/n)$, where n is the number of residues in the peptide. For CCE and CCK, $n = 39$ and $[\theta] = -35282$. ^b AUC was performed in PBS.

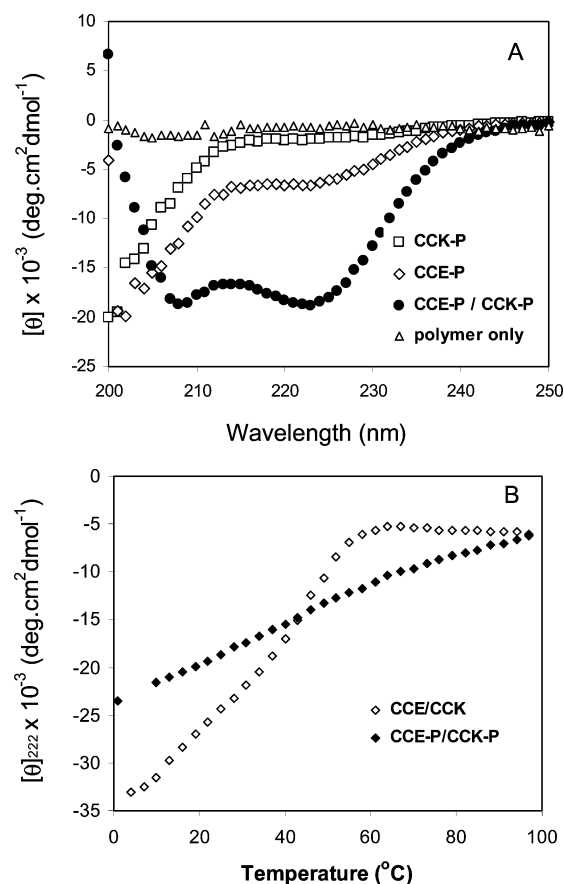


Figure 5. Characterization and thermal stability of HPMa graft copolymers. (A) CD spectra of CCE-P, CCK-P, and their equimolar mixture CCE-P/CCK-P. The spectra were recorded in PBS (50 mM Na₂HPO₄/NaH₂PO₄, 100 mM KCl, pH 7) with a peptide concentration of 100 μ M. (B) Temperature effect on the secondary structure of CCE/CCK and CCE-P/CCK-P in PBS as monitored by the change of molar ellipticity at 222 nm.

The association of the peptides was also investigated by CD measurements in aqueous solution containing 50% TFE (Figure 4B). The α -helical content of CCE, CCK, and CCE/CCK in PBS and in 50% TFE was calculated from the observed molar ellipticity at 222 nm according to the method developed by Chen et al.⁴³ The results of the quantitative analysis of CD spectra are shown in Table 2.

TFE has been widely used as a helix-inducing solvent to determine the potential of a given sequence to fold into a helix or to estimate the maximum helical content possible in the molecule.⁴⁴ It is also known that TFE disrupted hydrophobic interactions at the coiled-coil interface and stabilized the monomeric α -helix. As shown in Table 2, in the presence of 50% TFE, both CCE and CCK showed significant α -helix

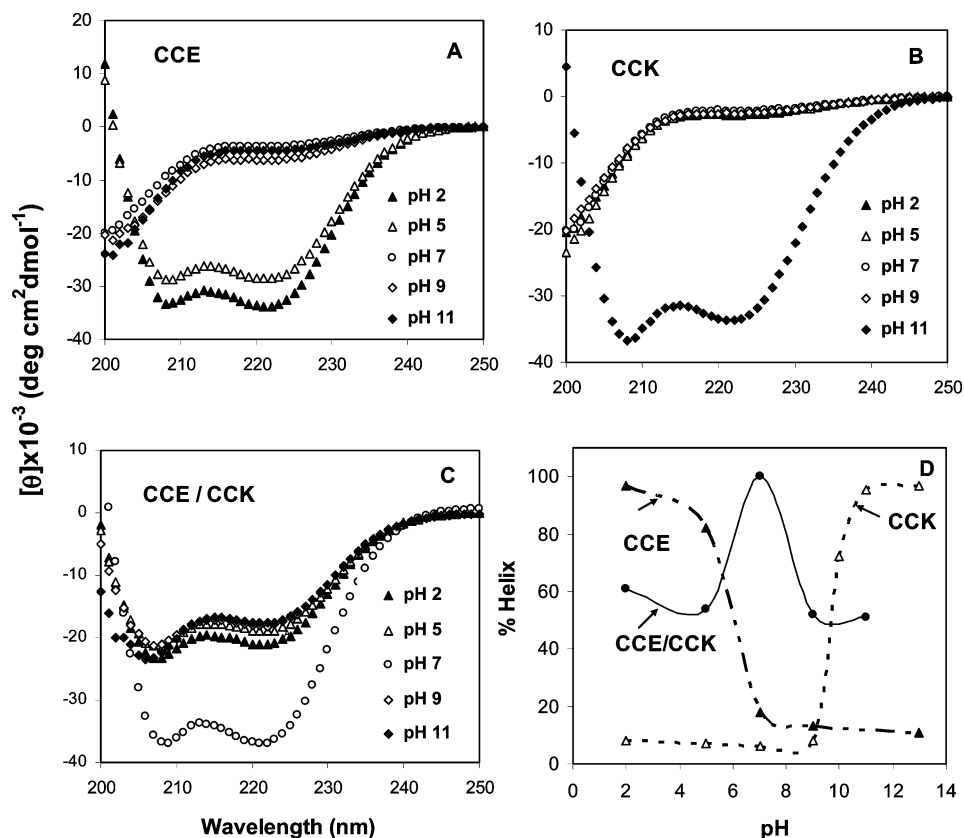


Figure 6. pH dependence of the secondary structure of (A) CCE, (B) CCK, and (C) CCE/CCK (1:1) and (D) the content of α -helix as a function of pH.

content, demonstrating that they had the potential to form highly helical structures under suitable conditions. On the contrary, CCE/CCK in PBS possessed a $[\theta]_{222}/[\theta]_{208}$ ratio of 1.0, whereas the value decreased in the presence of TFE to 0.79, indicative of a transition from heterodimers to monomeric α -helices.

Further studies revealed that the ratio of two oppositely charged peptides played an important role in the formation of the coiled-coil structure. At the stoichiometric equivalent ratio (50%) the lowest ellipticity at 222 nm was achieved, which corresponded to the existence of coiled-coil heterodimers (Figure 4C).

The secondary structure of peptide–polymer conjugates CCE–P, CCK–P, and CCE–P/CCK–P in neutral solution was examined using CD spectroscopy (Figure 5A). Similar tendencies to free peptides were found for the graft copolymers. Individual peptide–polymer conjugates CCK–P or CCE–P possessed predominately the random coil conformation. A typical feature of the coiled-coil structure was found when equivalents of CCE–P and CCK–P were mixed. This suggested that the association properties of the peptides were retained upon attachment to the HPMA copolymer backbone.

The thermal stability of the equivalent mixture of graft copolymers (CCE–P/CCK–P) was measured by monitoring the ellipticity at 222 nm under different temperatures. As shown in Figure 5B, the thermal stability of CCE–P/CCK–P increased compared with that of CCE/CCK. This observation may be explained by the stabilizing influence of the HPMA polymer backbone on the secondary structure of the peptide graft, which was reported by others.^{19,21}

Mechanism of Specificity. The present design strategy was to drive heterodimer formation by either electrostatic repulsion between two strands with the same charge or electrostatic attraction between two oppositely charged strands. Inspired by

O'Shea's work,²⁹ we investigated the stability of CCE and CCK at neutral pH as well as at acidic or alkaline pH values, respectively. If electrostatic destabilization of homodimers were dominant, the homodimers would be more stable when the charges were removed at extreme values of pH.

The pH effect on the structure of peptides CCK, CCE, and CCK/CCE is shown in Figure 6A–C. A transition from a random coil to a coiled-coil structure was detected when the pH was varied from 7 to basic for CCK or from 7 to acidic for CCE. The α -helical content dramatically changed for both CCE and CCK as the pH was varied from acidic to basic; the highest helical content was found at extreme pH values (Figure 4D, CCE at pH 2, CCK at pH 11). It correlated with the pK_a of the residues Glu ($pK_a = 4.5$) and Lys ($pK_a = 10.5$). At pH 4.5 and below, the Glu side chains were protonated and the stability of the coiled-coils increased. As the pH increased, progressive deprotonation of the Glu residues occurred, resulting in the dissociation of coiled-coil domains due to repulsive negative charges of the Glu carboxylic groups. A similar behavior was observed for CCK, when the pH changed from 7 to 11, with a correlation with the protonation of the amino groups of the lysine side chains.

A bell-shaped curve for the pH dependence of the α -helical content was found in CCE/CCK (Figure 6D). The highest helical content was observed at a neutral condition, where the heterodimer was the predominant molecular species. This finding was not surprising, since at acidic pH or basic pH, CCE or CCK, respectively, had a tendency to form homodimers, resulting in a decrease of ellipticity. Consequently, the apparent value of the α -helical content based on the calculation of the observed ellipticity was always higher for CCE/CCK than that of individual systems. In other words, the α -helical content was the homodimer's contribution from either CCK or CCE. At pH

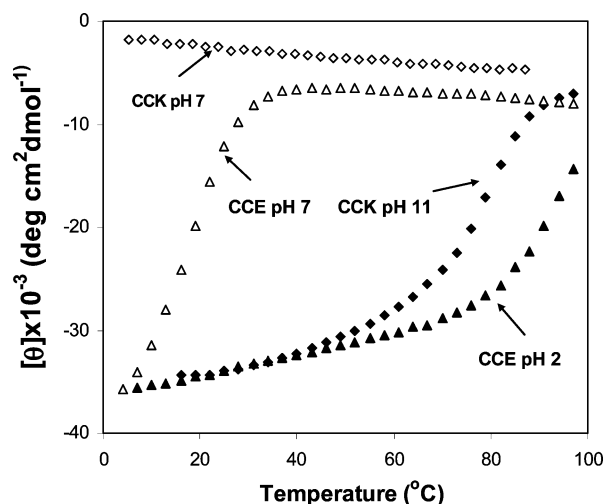


Figure 7. Thermal stability of CCE and CCK at different pH values.

7, the stabilizing electrostatic attraction between two different peptide strands was the strongest, and hence, the formation of heterodimers was thermodynamically favorable.

Very different thermal properties were displayed by CCE and CCK. As shown in Figure 7, the midpoint of the folding–unfolding transition of CCE was approximately 94 °C at pH 2 and about 20 °C at pH 7, indicating destabilization by negatively charged residues at neutral pH. It was remarkable that the midpoint of the folding–unfolding transition of CCK at pH 11 was close to 80 °C and that there was no folded structure at pH 7. The most likely explanation for the difference between CCE and CCK was that hydrogen bonds could form between a pair of carboxylic acids from side chains of Glu residues in the e and g' positions in the case of CCE, which resulted in the homodimeric association, although repulsive electrostatic interactions existed at neutral pH. However, hydrogen bonds were unable to form between a pair of primary amines from the side chain of lysine for CCK.

In summary, the finding that the stability of both homodimers was strongly pH dependent suggested that preferential heterodimer formation was driven primarily by repulsive electrostatic interactions among like charges. This conclusion agrees with studies on similar coiled-coil sequences reported in the literature.^{24,28,29}

Hybrid Hydrogel Self-Assembled from CCE–P/CCK–P. Coiled-coil self-assembly highly depends on environmental conditions such as concentration, temperature, pH, and the properties of the medium. To initiate the self-assembly process of hybrid hydrogels, HPMa graft copolymers were dissolved in PBS (50 mM Na₂HPO₄/NaH₂PO₄, 100 mM KCl, pH 7) in the concentration range of 0.1–1.0 wt % and incubated individually in the same buffer to equilibrate. Interestingly, it was observed that aqueous solutions of CCE–P or CCK–P alone did not form gels. In contrast, gel-like materials were found for all equimolar mixtures of CCE–P/CCK–P within the full concentration range tested.

The formation of hydrogel at a concentration of 0.1 wt % indicated a superior biorecognition of the two graft copolymers. This appeared to suggest that the self-assembly (gelation) was driven by the formation of heterodimers (and possibly higher order aggregates) that required both peptide–polymer conjugates CCE–P and CCK–P.

The self-assembly of HPMa graft copolymers was further evaluated by microrheology measurements (Figure 8). This

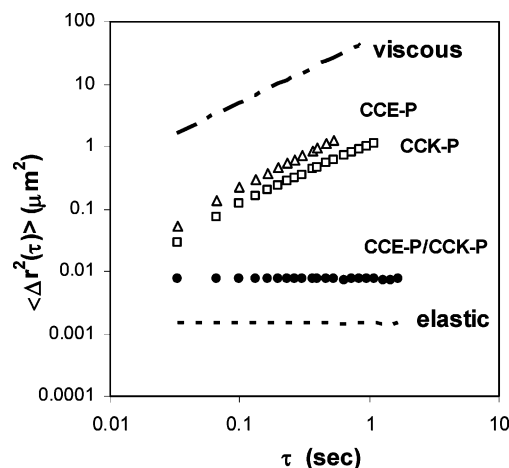
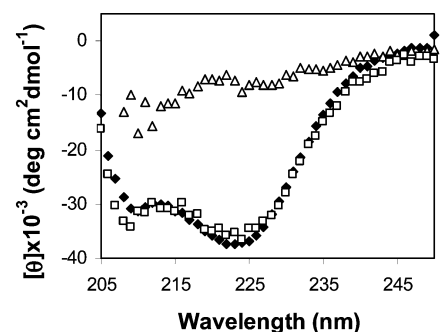


Figure 8. MSDs ($\langle \Delta r^2(\tau) \rangle$) of particles involved in CCE–P/CCK–P systems as a function of time (1% w/v).



◆ without GdnHCl ▲ 4 M GdnHCl denatured □ after dialysis

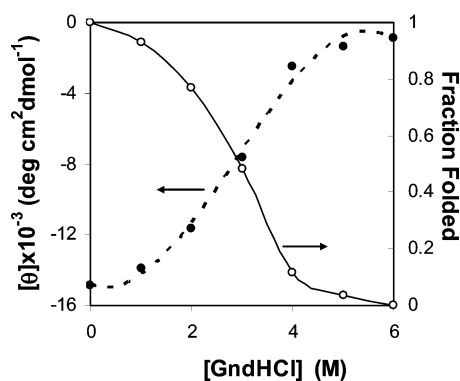


Figure 9. (A, top) CD spectra of the equimolar mixture CCK–P/CCE–P before (full tilted squares) and after (empty triangles) denaturation by guanidine hydrochloride at 25 °C with a 20 μ M peptide concentration and after removal of GdnHCl via dialysis (empty squares). (B, bottom) Dependence of the molar ellipticity at 222 nm of CCE–P/CCK–P on the concentration of GdnHCl.

technique relies on the measurement of thermally induced Brownian motion of micrometer-sized tracer particles dispersed in the samples.^{45,46} Mean-square displacement (MSD) of tracer particles increased linearly with time when the particles diffused freely in a liquid environment. However, MSD would reach a plateau over time when the motion of the particles was heavily restricted as in a gel-like environment. In our studies, the MSDs of graft copolymers containing CCE and CCK sequences were found to continuously increase with time, whereas that of the equimolar mixture of CCE–P and CCK–P remained constant. This result confirmed the formation of hybrid hydrogels and suggested that the gelation was modulated by CCE–P/CCK–P interactions (self-assembly).

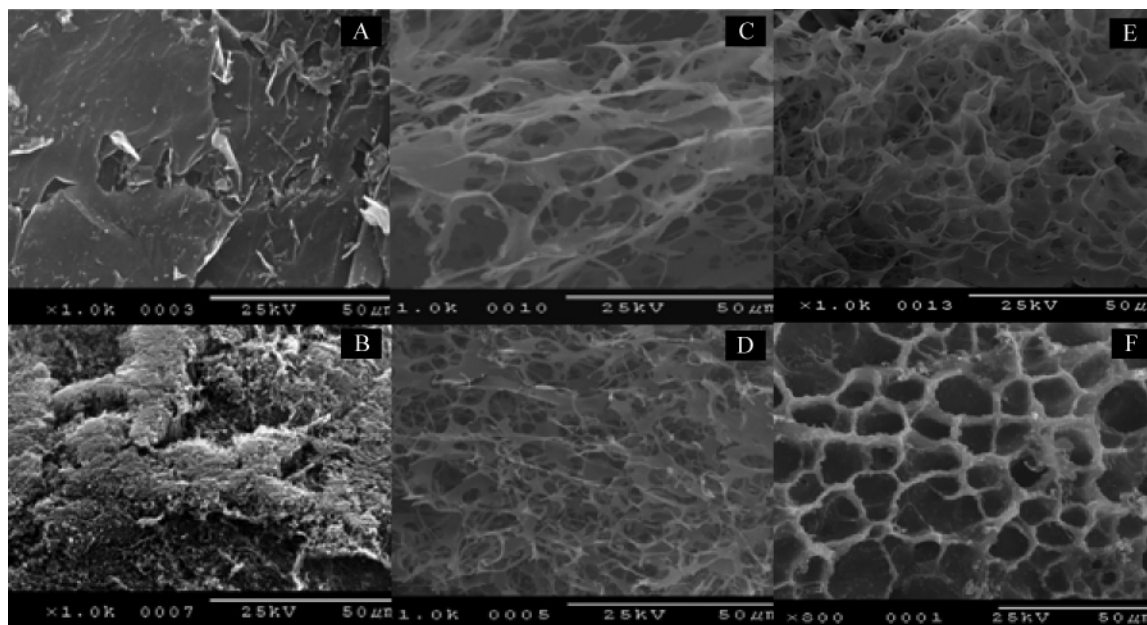


Figure 10. SEM images of hybrid hydrogels self-assembled from equimolar solutions of CCE-P and CCK-P in PBS: (A) 0.5 wt % HPMA copolymer solution; (B) one component (0.5 wt % CCE-P) only; (C) 0.1 wt % CCE-P/CCK-P; (D) 0.5 wt % CCE-P/CCK-P; (E) 1.0 wt % CCE-P/CCK-P; (F) 5.0 wt % CCE-P/CCK-P.

CCE-P/CCK-P formed coiled-coil heterodimers spontaneously when they were mixed together in PBS at neutral pH due to the electrostatic forces of the charged residues, which was confirmed by CD spectra. When CCE-P/CCK-P was incubated in concentrations from 0.1 to 1 wt % in PBS at room temperature, gel-like materials were observed at time periods from several hours to a whole day depending on the concentration. It was also found that when self-assembly of CCE-P/CCK-P was performed at a concentration of 0.5% in pure water, the gelation was visualized only after 3 days of incubation. This indicated that self-assembly of these materials was highly dependent on the solution conditions such as the concentration and the presence of salts. This is not surprising given the fact that the driving force of hydrogel formation—the coiled-coil assembly—is known to be affected by these factors.¹¹

An important observation was the *reversibility of self-assembly* after denaturation of the helical structure by a high concentration of GdnHCl. A self-assembled hydrogel was dissolved when a 6 M GdnHCl aqueous solution was added. The hydrogel reassembled after GdnHCl was removed by dialysis. This was presumably a consequence of the grafted α -helical coiled-coil reversible unfolding–folding process. CD spectroscopy was used to evaluate the stability of peptide–polymer conjugates in the presence of denaturing agent GdnHCl (Figure 9). It was found that CCE-P/CCK-P unfolded completely when exposed to 6 M GdnHCl in PBS at pH 7.0, which coincided with the disappearance of the gel-like structure in the presence of denaturant GdnHCl. The denatured coiled-coil structure refolded after removal of GdnHCl by dialysis. The denaturation midpoint was 3.0 M GdnHCl, which suggested that the heterodimerization domain has strong conformational stability.²³

Morphology of Freeze-Dried Self-Assembled Hydrogels.

The microstructure of hydrogels self-assembled from graft copolymer solutions of different concentrations was characterized using SEM and was found to be distinctly different from those of either the HPMA copolymer or the (unassembled) HPMA copolymer–peptide conjugate. Polymer samples showed a flat and tight texture when freeze-dried from H₂O solutions (Figure 10A,B). For hydrogel samples, the interaction of peptide

grafts led to a physically crosslinked polymer network that retained much water at the interior. After sublimation of the frozen water by lyophilization, pores or channels formed. The higher the concentration of the samples, the more intense the interaction between polymer chains with a concomitant increase of the level of organization of the structure. When the concentration of the graft copolymers in the samples increased from 0.1 to 5 wt %, the morphology changed from a leaflike to a spongelike structure (Figure 10C–F).

Conclusions

A novel hybrid hydrogel system whose self-assembly was mediated by the formation of heterodimeric antiparallel coiled-coils was designed. A pair of oppositely charged peptides with 39 amino acid residues, CCE and CCK, were rationally designed, synthesized, and covalently attached to the hydrophilic HPMA copolymer backbone. CD and AUC experiments indicated pH-dependent behavior of CCE and CCK. At neutral pH, each individual peptide possessed a random coil structure, but folded into homodimeric coiled-coils at low and high pH, respectively. However, a heterodimeric coiled-coil structure was observed when the two peptides were mixed equimolarly at neutral pH. These associating properties were retained in the graft copolymers. Consequently, the graft copolymers CCE-P/CCK-P were observed to self-assemble into hydrogels in PBS solution at neutral pH at concentrations as low as 0.1 wt %. Moreover, the reversibility of the hybrid hydrogel self-assembly was evaluated by denaturation of the helical structure with guanidine hydrochloride.

The application of a two-component self-assembling system can be broadened to cover a wide range of in situ forming hybrid hydrogels as peptide, protein, and gene delivery systems, since the storage of the components and their self-assembly occur in aqueous media. This approach could also potentially be used to join noncompatible macromolecules, such as hydrophilic molecules and liquid crystal hydrophobic muscle mimic,⁴⁷ without the need to use a third, compatibility-providing, component. The properties of a particular system may be fine-

tuned by the choice of the synthetic backbone and the structure and content of peptide grafts. In addition to drug delivery, these systems may find application in biosensors, affinity separations, and nanoreactors. As illustrated in this paper as well as other papers,^{40,48,49} the knowledge of the biorecognition of antiparallel coiled-coil heterodimers and/or other arrangements of peptide building blocks may lead, in the future, to a new area of biomaterials design.

Acknowledgment. We thank Drs. Pavla Kopečková and Bruce Yu for valuable discussions and Jon Callahan for critical reading of the manuscript. The research was supported in part by NIH Grant EB005288.

Note Added after ASAP Publication. This paper was released ASAP on 3/9/2006. Figure 4 was modified. The correct version was posted on 3/14/2006.

References and Notes

- Rajagopal, K.; Schneider, J. P. *Curr. Opin. Struct. Biol.* **2004**, *14*, 480–486.
- Zhang, S. *Biotechnol. Adv.* **2002**, *20*, 321–339.
- MacPhee, C. E.; Woolfson, D. N. *Curr. Opin. Solid State Mater. Sci.* **2004**, *8*, 141–149.
- Vandermeulen, G. W.; Klok, H. A. *Macromol. Biosci.* **2004**, *4*, 383–398.
- Lutolf, M. P.; Hubbell, J. A. *Nat. Biotechnol.* **2005**, *23*, 47–55.
- Ehrick, J. D.; Deo, S. K.; Browning, T. W.; Bachas, L. G.; Madou, M. J.; Daunert, S. *Nat. Mater.* **2005**, *4*, 298–302.
- Langer, R.; Tirrell, D. A. *Nature* **2004**, *428*, 487–492.
- Zhang, S. G.; Marini, D. M.; Hwang, W.; Santoso, S. *Curr. Opin. Chem. Biol.* **2002**, *6*, 865–871.
- Collier, J. H.; Messersmith, P. B. *Bioconjugate Chem.* **2003**, *14*, 748–755.
- Kim, U. J.; Park, J.; Li, C.; Jin, H. J.; Valluzzi, R.; Kaplan, D. L. *Biomacromolecules* **2004**, *5*, 786–792.
- Yu, Y. B. *Adv. Drug Delivery Rev.* **2002**, *54*, 1113–1129.
- Lupas, A. *Trends Biochem. Sci.* **1996**, *21*, 375–382.
- Burkhard, P.; Stetefeld, J.; Strelkov, S. V. *Trends Cell Biol.* **2001**, *11*, 82–88.
- Petka, W. A.; Harden, J. L.; McGrath, K. P.; Wirtz, D.; Tirrell, D. A. *Science* **1998**, *281*, 389–392.
- Wang, C.; Stewart, R. J.; Kopeček, J. *Nature* **1999**, *397*, 417–420.
- Kopeček, J.; Tang, A. J.; Wang, C.; Stewart, R. J. *Macromol. Symp.* **2001**, *174*, 31–42.
- Vandermeulen, G. W. M.; Tziatzios, C.; Duncan, R.; Klok, H. A. *Macromolecules* **2005**, *38*, 761–769.
- Xu, C.; Breedveld, V.; Kopeček, J. *Biomacromolecules* **2005**, *6*, 1739–1749.
- Vandermeulen, G. W. M.; Tziatzios, C.; Klok, H. A. *Macromolecules* **2003**, *36*, 4107–4114.
- Stevens, M. M.; Allen, S.; Davies, M. C.; Roberts, C. J.; Sakata, J. K.; Tendler, S. J.; Tirrell, D. A.; Williams, P. M. *Biomacromolecules* **2005**, *6*, 1266–1271.
- Pechar, M.; Kopečková, P.; Joss, L.; Kopeček, J. *Macromol. Biosci.* **2002**, *2*, 199–206.
- Woolfson, D. N. *Adv. Protein Chem.* **2005**, *70*, 79–112.
- Chao, H.; Bautista, D. L.; Litowski, J.; Irvin, R. T.; Hodges, R. S. *J. Chromatogr., B: Biomed. Sci. Appl.* **1998**, *715*, 307–329.
- Litowski, J. R.; Hodges, R. S. *J. Biol. Chem.* **2002**, *277*, 37272–37279.
- Oakley, M. G.; Hollenbeck, J. J. *Curr. Opin. Struct. Biol.* **2001**, *11*, 450–457.
- McClain, D. L.; Woods, H. L.; Oakley, M. G. *J. Am. Chem. Soc.* **2001**, *123*, 3151–3152.
- Su, J. Y.; Hodges, R. S.; Kay, C. M. *Biochemistry* **1994**, *33*, 15501–15510.
- Myszka, D. G.; Chaiken, I. M. *Biochemistry* **1994**, *33*, 2363–2372.
- O'Shea, E. K.; Lumb, K. J.; Kim, P. S. *Curr. Biol.* **1993**, *3*, 658–667.
- Hodges, R. S. *Biochem. Cell Biol.* **1996**, *74*, 133–154.
- Pack, P.; Müller, K.; Zahn, R.; Plückthun, A. *J. Mol. Biol.* **1995**, *246*, 28–34.
- Tang, A.; Kopeček, J. *Biomacromolecules* **2002**, *3*, 421–431.
- Stevens, M. M.; Flynn, N. T.; Wang, C.; Tirrell, D. A.; Langer, R. *Adv. Mater.* **2004**, *16*, 915–918.
- Wang, C.; Kopeček, J.; Stewart, R. J. *Biomacromolecules* **2001**, *2*, 912–920.
- Yang, J.; Xu, C.; Kopečková, P.; Kopeček, J. *Macromol. Biosci.*, in press.
- Kopeček, J.; Bažilová, H. *Eur. Polym. J.* **1973**, *9*, 7–14.
- Starcher, B. *Anal. Biochem.* **2001**, *292*, 125–129.
- Ellman, G. L. *Arch. Biochem. Biophys.* **1959**, *82*, 70–77. Gergel, D. L.; Cederbaun, A. I. *Biochemistry* **1996**, *35*, 16186–16194.
- Laue, T. M.; Shah, B. D.; Ridgeway, T. M.; Pelletier, S. L. In *Ultracentrifugation in Biochemistry and Polymer Science*; Harding, S. E., Rowe, A. J., Horton, J. C., Eds.; The Royal Society of Chemistry: Cambridge, U.K., 1992; p 90.
- Ryadnov, M. G.; Woolfson, D. N. *J. Am. Chem. Soc.* **2005**, *127*, 12407–12415.
- Crocker, J. C.; Valentine, M. T.; Weeks, E. R.; Gisler, T.; Kaplan, P. D.; Yodh, A. G.; Weitz, D. A. *Phys. Rev. Lett.* **2000**, *85*, 888–891.
- Oakley, M. G.; Kim, P. S. *Biochemistry* **1998**, *37*, 12603–12610.
- Chen, Y. H.; Yang, J. T.; Chau, K. H. *Biochemistry* **1974**, *13*, 3350–3359.
- Nelson, J. W.; Kallenbach, N. R. *Proteins* **1986**, *1*, 211–217.
- Mason, T. G.; Weitz, D. A. *Phys. Rev. Lett.* **1995**, *74*, 1250–1253.
- Levine, A. J.; Lubensky, T. C. *Phys. Rev. Lett.* **2000**, *85*, 1774–1777.
- Li, M.-H.; Keller, P.; Yang, J.; Albouy, P.-A. *Adv. Mater.* **2004**, *16*, 1922–1925.
- Pandya, M. J.; Spooner, M. G.; Sunde, M.; Thorpe, J. R.; Rodger, A.; Woolfson, D. N. *Biochemistry* **2000**, *39*, 8728–8734.
- Zhou, M.; Bentley, D.; Ghosh, I. *J. Am. Chem. Soc.* **2004**, *126*, 734–735.

BM051002K